GEOMORPHOMETRY 2021
PERUGIA, ITALY
PARTNERS SPONSORS
SEPT 13 - 17 2021

# Evaluation of slopes calculated from TanDEM-X digital elevation models at 3 spatial resolutions

Peter L. Guth[§], Morgan E. Kane
Department of Oceanography
United States Naval Academy
572C Holloway Road
Annapolis MD 21402 USA
pguth@usna.edu, morgan3kane@gmail.com

*Abstract*—**The three resolutions of the TanDEM-X DEM show the effects of resolution on calculated slopes. We compare those slopes with independently derived lidar DEMs at the same spatial resolutions (0.4, 1, and 3 arc seconds). The TanDEM-X 0.4 arc second DEM shows significant differences from lidar derived DEMs at the same resolution, and generally has more variability which may be due to radar speckle, while the 1 and 3 second DEMs have very similar slope characteristics as the lidar DEMs. The slopes decrease as the DEM spacing increases, but the rate of decrease does not vary systematically. Slopes all increase with latitude.**

## I. INTRODUCTION

Slope is one of the most important applications for digital elevation models (DEMs), as well as one of the best ways to assess the quality of a DEM because derivative grids amplify any errors. Slope computed from a DEM depends on the grid spacing, and the TanDEM-X [1] offers three resolutions of a radar-derived DEM and the ability to assess how slope decreases with grid size. We used lidar point clouds to create matching digital terrain models (DTMs) and digital surface models (DSMs) to assess the accuracy of the TanDEM-X slopes.

## II. METHODS

We applied for 6 TanDEM-X data sets for this research project, and selected test regions to look at low and high latitudes to see the effects of the variable ratio of the DEM spacing in meters, and to test various landforms. All test regions have lidar data with 1-10 points/m², meaning that the DEMs created from them averaged approximately 100-1000 lidar returns per grid cell for the 0.4" grids, and 800-80000 returns for the 3" grids.

Three data sets allow categorization of the landscape at a scale appropriate for these test areas. Figure 1 shows relief classification [2,3] at 1 km resolution for the 6 six study areas, and that the six are noticeably different. Figure 2 shows geomorphons [4, 5, 6] at the same scale, with two pairs of similar characteristics (Blue Ridge/Canyon Mountains, and Guam/Norway). We excluded the plains category, which includes the ocean in this data set [6] because our test areas had no actual plains. Figure 3 shows the 300 m landcover [7, 8], and that all test areas are different. The diagrams show that these test regions sample a variety of landforms and the specific categories are less important; versions of these figures are available on the web with legends.

**Table 1.** Study areas.

| Test area | Center Location | Area km² | Lidar Points (billions) | Lidar density (pts/m²) | TanDEM-X x/y Spacing |
|---|---|---|---|---|---|
| Blue Ridge | N38.712° W78.282° | 241.38 | 2.06 | 9.2 | 0.783 |
| Canyon Mtns | N39.355° W112.23° | 122.81 | 0.41 | 3.4 | 0.776 |
| El Hiero | N27.740° W18.019° | 274.77 | 0.58 | 1.3 | 0.890 |
| Guam | N13.295° E144.703° | 144.05 | 1.13 | 6.4 | 0.979 |
| Norway | N58.252° E7.559° | 1213.79 | 4.61 | 11.8 | 0.791 |
| Oahu | N21.491° W158.187° | 54.11 | 0.17 | 3.1 | 0.936 |

We created independent DTMs and DSMs from lidar point clouds from the national mapping agencies in Norway, Spain, and the United States, matching the resolution of the TanDEM-X DEMs at 0.4", 1", and 3", with the data set in Norway having a longitudinal spacing 1.5 times the latitudinal spacing. For the DTM we used the elevation at the 5$^{th}$ percentile of all points falling within the cell, and for the DSM we used the elevation at the 95$^{th}$ percentile; these choices removed any noise not recognized in the lidar point cloud processing. The lidar DEMs use all points imaged by the laser beam, and include the effects of sloping terrain and features like vegetation above the ground.

We computed slopes for 9 DEMs for each test area (Figure 4), using the arc second data without reinterpolation because an appropriate algorithm can correctly compute slope [9, 10]. The figure shows the average data spacing in meters along the x axis, because that spacing corresponds to a UTM grid that would give equivalent statistics [10]. Table 1 shows the ratio between the x and y spacing with the arc second DEMs, and the degree to which the pixels are not square.

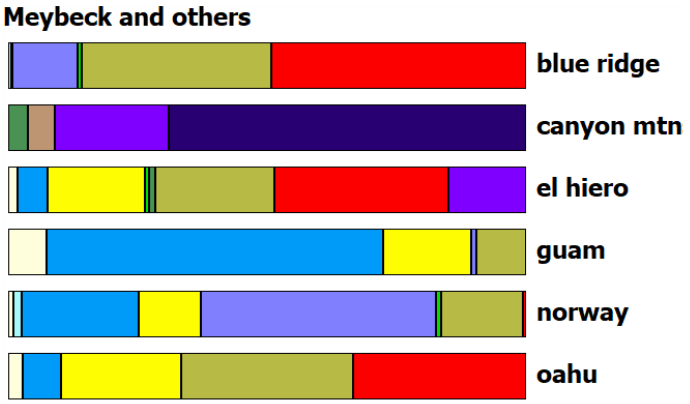


**Figure 1.** Relief classification (1 km resolution; [2,3]). [Hi-res on web with legend]

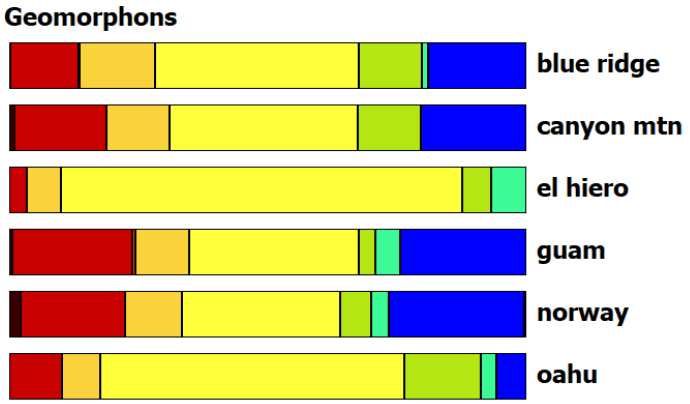


**Figure 2.** Geomorphon (1 km resolution; [4,5,6]) categories. [Hi-res on web with legend]

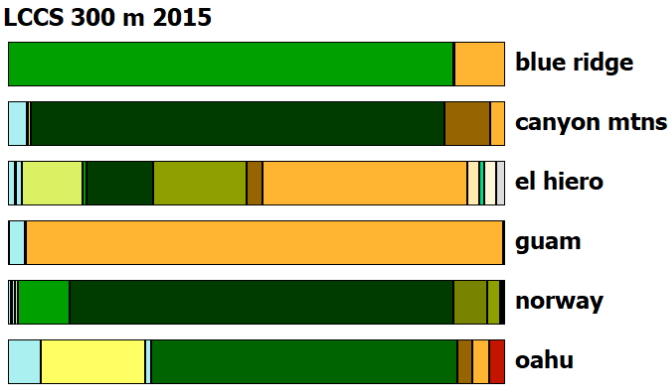


**Figure 3.** -Land cover categories (300 m resolution [7,8]). [Hi-res on web with legend]

## IV. RESULTS

Figure 4 shows portions of the slope maps for the 9 DEMs of El Hiero. At each scale, the maps are broadly similar and show similar patterns. As the grid spacing increases, there are fewer points in the DEM: the 0.4" grid has 56 times more points compared to the 3" grid. This results in smoothing of the map, with lower slope values and less detail.

Figure 5 shows the mean slope and slope standard deviation for the 6 areas. In all cases the lidar DTM has slightly smaller values both for slope and slope variation than the lidar DSM, reflecting the smoother nature of the ground surface DTM.

The 0.4" DEMs show the greatest variability, both for the mean slope and slope standard deviation.

For all three resolutions, the El Hiero TanDEM-X has steeper average slopes, and lower slope standard deviation. For the other 5 areas, slope standard deviation at 1" and 3" spacing is very similar for all three DEMs, and much greater at 0.4" spacing which might reflect greater "noise" with small scale features, and perhaps also radar speckle for the TanDEM-X.

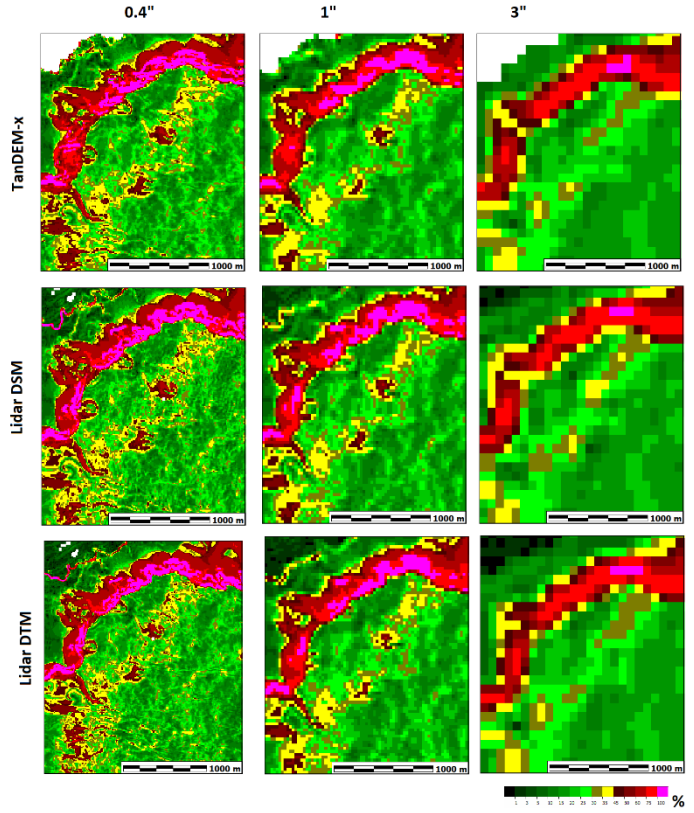


**Figure 4.** -Slope maps for a portion of the El Hiero study area. [Hi-res on web]

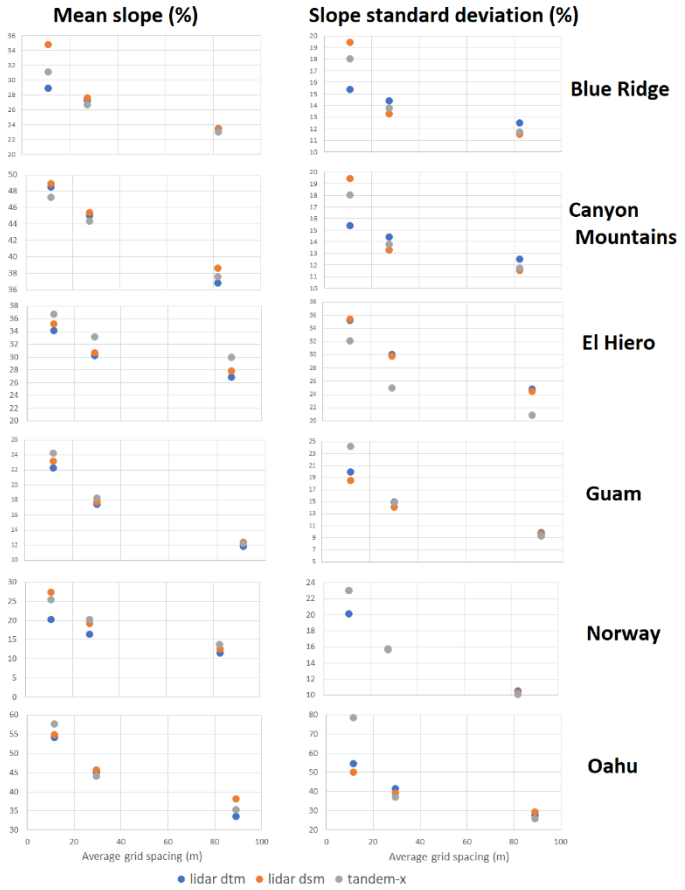


**Figure 5.** Mean slope and slope standard deviation. Vertical scales different on all graphs. [Hi-res]

In a lidar point cloud, the points in a grid cell that contribute to a DEM posting will have a lower bound at the ground surface, and an upper bound at the top of the vegetation canopy or manmade features. Figure 6 shows the terrain elevation variation for a range of DEM grid sizes and slopes, assuming the aspect occurs along the diagonals of the grid; if the aspect if N-S or E-W, it will be smaller by a factor of √2. In flat terrain almost all of the variation results from the vegetation canopy, whereas in steeper terrain, depending on the vegetation height the sloping ground has a much greater influence.

For a DEM derived from radar like TanDEM-X or an optical sensor, the surface imaged by the sensor will resemble a DSM with the possibility for some penetration into vegetation depending on the season, canopy density, and sensor characteristics.

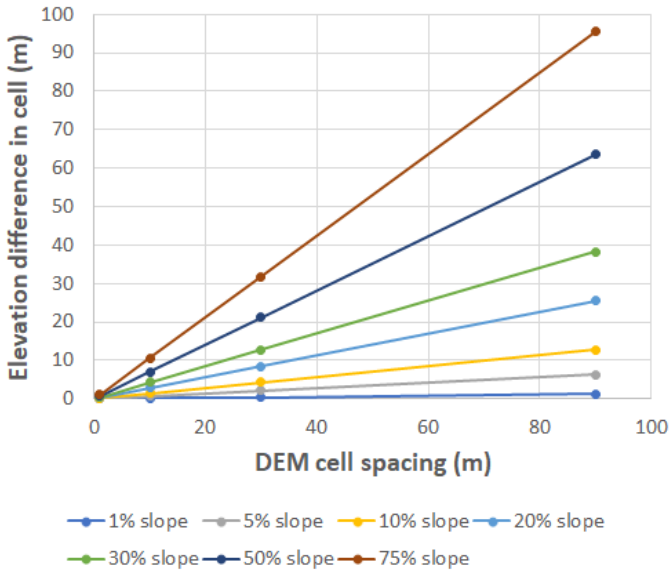


**Figure 6.** Elevation variation within grid cell spacing as a function of slope.

Slope does not depend on the absolute elevations, but on the relative relief of the points surrounding each grid node. If the DTM and DSM were parallel, the slopes derived from each would be identical. Slope does depend on latitude, because the size of the geographic pixels decreases with latitude and slope is a function of the average dimensions in meters of geographic pixels. We created DEMs from each of our test areas from the lidar, with pixel spacing corresponding to moving the lidar point cloud to different latitudes (Figure 7). These show that for the same topography represented by locations in a UTM projection and placed in a grid with the dimensions of a 1" pixel, the slopes will be greater at higher latitudes. The rate of change is not consistent, and may reflect anisotropy in the terrain. The dy component of slope will not change if the terrain is shifted in latitude, but the dx component will change.

## V. Discussion & Conclusion

All 6 test areas are in moderately steep terrain, with average slopes ranging from 23% to 55% (13-29°) at the 0.4" scale, and 10% to 25% (6-14°) at 3" scale. DEMs typically have different characteristics in mountainous and floodplain regions, and many assessments of DEM accuracy have focused on one terrain type or the other.

The 3" TanDEM-X compared favorably with SRTM and MERIT in floodplains [11], but proved to be less accurate in steeper terrain [12, 13, 14]. The 0.4" TanDEM-X met its mission specification for absolute deviation, but the errors increased with slopes above 10° and in forested regions [12].

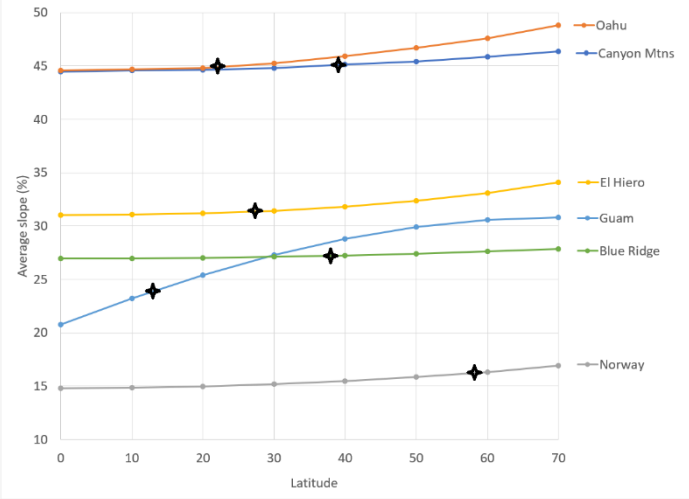


**Figure 7.** Average slopes the 1" lidar DEMs for the test areas shifted to different latitudes. Black symbols show the latitude of each test area.

The TanDEM-X has a number of limitations: alone among the global DEMs at 1-3" spacing, it references elevations to the ellipsoid instead of the geoid; it has not been hole filled; it has not had the oceans cleaned; and it has various anomalies on land areas.

Our assessment used lidar to create DEMs with the same resolution as the TanDEM-X, in contrast to methods that use a very high resolution lidar DEM (1 m resolution) and resampled the lower resolution data to 1 m [15]. The resampled 1 m data will be smoother and lack the detail in the true 1 m DEM.

Slope decreases with increasing DEM grid spacing, but the rate of decrease varies for each of the 6 test areas and the decrease does not occur in a systematic fashion. Landcover and landforms must affect the horizontal scale of slope variations, but the variability shown in Figures 1-3 shows complexity in the relationship. For arc second DEMs latitude generally has a small impact on average slopes; the effect is generally small, but is much more significat

## VI. ACKNOWLEDGMENTS

We thank DLR for providing the 0.4" and 1" TanDEM-X data used for this research. All computations were done with MICRODEM [16]. Higher resolution copies of the graphics are available on the internet by clicking the links in the figure captions.

## REFERENCES

[1] Rizzoli, P., Martone, M., Gonzalez, C., Wecklich, C., Borla Tridon, D., Brautigam, B., Bachmann, M., Schulze, D., Fritz, T., Huber, M., Wessel, B., Krieger, G., Zink, M., & Moreira, A. (2017). Generation and performance assessment of the global TanDEM-X digital elevation model. ISPRS Journal of Photogrammetry and Remote Sensing, Vol 132, pp. 119-139.

[2] Meybeck, M., Green, P., and Vörösmarty, C., 2001, A new Typology for mountains and other relief classes: Mountain Research and Development, 21(1), 34-45, https://doi.org/10.1659/0276-4741(2001)021[0034:ANTFMA]2.0.CO;2

[3] Reuter, H., and Nelson, 2008, Landform Classification: European Soil Data Science Center, Joint Research Center, https://esdac.jrc.ec.europa.eu/projects/landform-classification

[4] Jasiewicz, J., Stepinski, T., 2013, Geomorphons - a pattern recognition approach to classification and mapping of landforms, Geomorphology, vol. 182, 147-156. https://doi.org/10.1016/j.geomorph.2012.11.005

[5] Amatulli, G., Domisch, S., Tuanmu, MN. et al. A suite of global, cross-scale topographic variables for environmental and biodiversity modeling. Sci Data 5, 180040 (2018). https://doi.org/10.1038/sdata.2018.40

[6] http://www.earthenv.org/topography has 1 km geomorphons

[7] ESA. Land Cover CCI Product User Guide Version 2. Tech. Rep. (2017). Available at http://maps.elie.ucl.ac.be/CCI/viewer/download/ESACCI-LC-Ph2-PUGv2_2.0.pdf

[8] http://maps.elie.ucl.ac.be/CCI/viewer/download.php has 2015 300 m land cover

[9] Strobl, P., Conrad Bielski, Peter Guth, Carlos Grohmann, Jan-Peter Muller, Carlos López-Vázquez, Dean B. Gesch, Giuseppe Amatulli, Serge Riazanoff, Claudia Carabajal. (2021). The Digital Elevation Model Intercomparison eXperiment DEMIX, a community based approach at global DEM benchmarking: International Archives of the Photogrammetry, Remote Sensing and Spatial Information Sciences, Proceedings of the 2021 edition of the XXIVth ISPRS Congress.

[10] Guth, P.L, and Kane, M.E., 2021 Slope, Aspect, and Hillshade Algorithms for Non-Square Digital Elevations Models: Transactions in GIS, in press.

[11] Hawker, L., Neal, J., and Bates, P., 2019, Accuracy assessment of the TanDEM-X 90 Digital Elevation Model for selected floodplain site s: Remote Sensing of Environment, Volume 232, 111319,https://doi.org/10.1016/j.rse.2019.111319

[12] Gdulová, K., Marešová, J., and Moudrý, V., 2020, Accuracy assessment of the global TanDEM-X digital elevation model in a mountain environment: Remote Sensing of Environment, Volume 241, 111724, https://doi.org/10.1016/j.rse.2020.111724

[13] Altunel, A.O., 2019, Evaluation of TanDEM-X 90 m Digital Elevation Model: International Journal of Remote Sensing, 40:7, 2841-2854 , https://doi.org/10.1080/01431161.2019.1585593

[14] Altunel, A.O., 2020, Questioning the effects of raster-resampling and slope on the precision of TanDEM-X 90 m digital elevation model, Geocarto International,DOI: 10.1080/10106049.2020.1840636

[15] Uuemaa, E., Ahi, S., Montibeller, B., Muru, M., and Kmoch, A., . 2020. Vertical accuracy of freely available global digital elevation models (ASTER, AW3D30, MERIT, TanDEM-X, SRTM, and NASADEM): *Remote Sens.* 12, no. 21: 3482. https://doi.org/10.3390/rs12213482.

[16] Guth, P.L., 2009, Geomorphometry in MICRODEM, In Hengl, T., Reuter, H.I. (eds), Geomorphometry: concepts, software, applications. Developments in Soil Science Series, Elsevier, p.351-366. Program at https://www.usna.edu/Users/oceano/pguth/website/microdem/microdemdown.htm